Chinese Chemical Letters 35 (2024) 108494

Contents lists available at ScienceDirect

Chinese Chemical Letters

journal homepage: www.elsevier.com/locate/cclet

A shape-reconfigurable, light and magnetic dual-responsive shape-memory micropillar array chip for droplet manipulation

Wen-Qi Ye, Wen-Xin Fu, Xiao-Peng Liu, Chun-Guang Yang, Zhang-Run Xu*

Research Center for Analytical Sciences, Northeastern University, Shenyang 110819, China

ARTICLE INFO

Article history:
Received 15 November 2022
Revised 4 April 2023
Accepted 20 April 2023
Available online 22 April 2023

Keywords:
Microfluidics
Droplet manipulation
Micropillar array
Shape memory polymer
Magnetic response
Light response

ABSTRACT

Droplet manipulation on an open surface has great potential in chemical analysis and biomedicine engineering. However, most of the reported platforms designed for the manipulation of water droplets cannot thoroughly solve the problem of droplet evaporation. Herein, we report a shape-reconfigurable micropillar array chip for the manipulation of water droplets, oil droplets and water-in-oil droplets. Water-in-oil droplets provide an enclosed space for water droplets, preventing the evaporation in an open environment. Perfluoropolyether coated on the surface of the chip effectively reduces the droplet movement resistance. The micropillar array chip has light and magnetic dual-response due to the Fe_3O_4 nanoparticles and the reduced iron powder mixed in the shape-memory polymer. The micropillars irradiated by a near-infrared laser bend under the magnetic force, while the unirradiated micropillars still keep their original shape. In the absence of a magnetic field, when the micropillars in a temporary shape are irradiated by the near-infrared laser to the transition temperature, the micropillars return to their initial shape. In this process, the surface morphology gradient caused by the deformation of the micropillars and the surface tension gradient caused by the temperature change jointly produce the driving force of droplet movement.

Droplet manipulation on an open surface is a unique technique of droplet microfluidics [1]. It retains the advantages of traditional microfluidic chips, such as low sample consumption, and high mass and heat transfer efficiency. Besides, it has some other advantages of simple preparation and easy integration. Individual droplet manipulation on open surfaces has attracted wide attention because of its potential application in chemistry, environment, and biomedicine [2]. Electrowetting-on-dielectric [3], thermocapillary force [4,5], surface morphology gradient [6,7], and magnetic force [8] have been used for droplet manipulation on open surfaces. No matter what strategy, the directional transport of droplets is realized by directly or indirectly utilizing the imbalanced surface tension of droplets.

Shape memory polymer can be restored from temporary programmed shape to original shape under the stimulation of the external environment (such as temperature, electric field, magnetic field, and light) [9]. The microfluidic chip made of shape memory polymer has stimulus-response, which makes it a carrier as well as an actuator. There are a few studies on stimulus-responsive polymers used in microfluidic chips, mainly focusing on switchable wetting [10–13] and fluid manipulation [6,7,14–16]. However, the deformation process of most stimulus-responsive microfluidic chips is irreversible, and the programming of temporary shapes often requires external pressure, which will inevitably limit the popularization of stimulus-responsive materials in the field of microfluidics. Two-way shape memory polymers can reversibly and spontaneously switch between temporary shape and initial shape with the change of external conditions, and they have potential application value in biomedicine, sensors, actuators, and other fields [17,18]. Both semi-crystalline polymer and liquid crystal elastomer exhibit reversible shape memory based on temperature response [17]. Generally speaking, the trigger temperature of the reversible shape change of these two-way polymers is either too high or too low, which limits the application range of shape memory polymers.

Magnetically responsive shape memory polymers have broad application prospects because of their advantages, such as remote non-contact control, fast response speed, and strong penetrating power [19,20]. In this work, we fabricated a shape-memory micropillar array chip for droplet manipulation using ethylene-vinyl acetate copolymer (EVA) with photothermal and magnetic responses. The perfluoropolyether coating on the surface of the micropillar array chip can effectively reduce the droplet movement resistance for readily manipulating the water droplets and

* Corresponding author.
E-mail address: xuzr@mail.neu.edu.cn (Z.-R. Xu).

https://doi.org/10.1016/j.cclet.2023.108494
1001-8417/

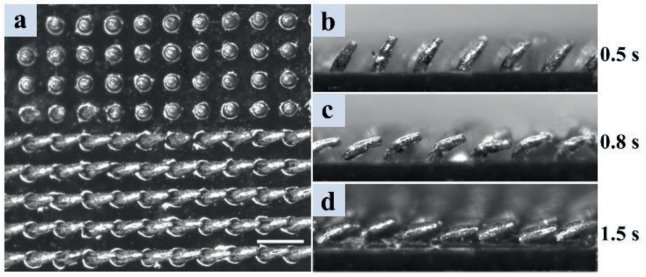

Fig. 1. Microscopic images of bent micropillars. (a) Bent micropillars after irradiated by NIR in the magnetic field (bottom) and unchanged micropillars without irradiation (top). Scale bar, 300 μm. (b-d) Micropillars with different bending angles obtained by controlling NIR laser irradiation time.

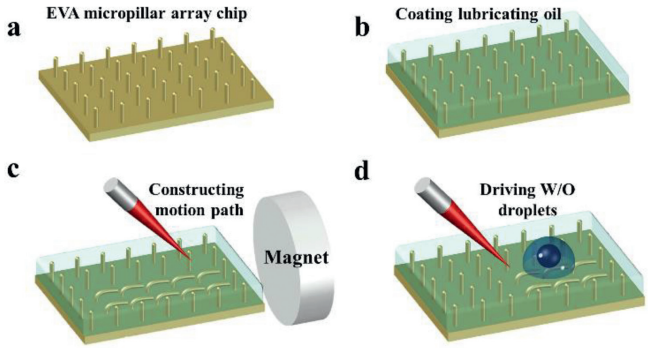

Fig. 2. Schematic diagram of droplet manipulation. (a) EVA micropillar array chip. (b) Coating perfluoropolyether as a lubricating layer on the surface of the EVA micropillar array. (c) Constructing the droplet motion path by irradiating the micropillar array with NIR laser in a magnetic field. (d) Driving the W/O droplets through NIR laser irradiation to restore the shape of the micropillars.

oil droplets. The micropillars in a specific area can be shaped by near-infrared light irradiation in the magnetic field to construct the droplet control path. The NIR laser triggered micropillar deformation has the advantages of non-contact and flexible adjustment driven by light, and its essence is the thermal response. Water-in-oil (W/O) droplets can avoid the droplet damage caused by temperature rise. The droplet movement path can be flexibly constructed on the chip surface, and the chip can be reused.

Fe_3O_4 NPs are among the most widely used magnetic particles because of their biocompatibility, non-toxicity, ease of large-scale synthesis, and strong magnetism [21]. In addition, they are also used as a photothermal material for tumor treatment [22]. In this study, the EVA micropillar array chip was doped with Fe_3O_4 NPs and reduced iron powder. The Fe_3O_4 NPs are uniformly distributed in the whole chip, while the reduced iron powder only exists in the micropillars. Before thermoforming, the PDMS micro-pit array mold was filled with reduced iron powder (Figs. S1a and b in Supporting information). In the first stage of thermoforming (135 °C), EVA composites melted and flowed into the micro-pits to wrap the reduced iron powder. In the second stage (200 °C), high temperature triggered dicumyl peroxide to release free radicals to induce EVA crosslinking (Fig. S1c). After cooling and demoulding, a micropillar array with the reduced iron powder was obtained (Fig. S1d), and the magnetic response ability of the micropillars was enhanced. Thus, the micropillar array prepared with the EVA composite has both photothermal response and magnetic response.

The micropillars will not be deformed by magnetic force in the magnetic field without irradiation. When NIR laser irradiated the micropillars in the magnetic field, the temperature of the micropillars rose to the transition temperature and the micropillars became soft. Then the micropillars bent under the action of magnetic force. The magnetic field was maintained until the micropillar temperature dropped below the transition temperature, and the micropillars was fixed in a temporary shape. When the curved micropillars were irradiated with NIR laser again, the micropillar temperature rose to the transition temperature and the micropillars returned to their original shape (Video S1 in Supporting information). Fig. 1a shows that the micropillars bend when irradiated by NIR laser in the magnetic field, while the micropillars in the unirradiated area remains unchanged in shape. In addition, the bending degree of the micropillars can be controlled by changing NIR laser irradiation time (Figs. 1b–d).

Perfluoropolyether is a lubricating oil with low surface energy and good chemical and biological inertness for preparing liquid-infused surfaces (LIS) [23]. In this work, LIS was constructed by coating perfluoropolyether on the surface of the micropillar array for reducing the friction between droplets and the surface [24] (Figs. 2a and b). Then, the droplet motion path can be constructed by scanning the chip surface with a NIR laser in the magnetic field. Then the NIR laser scans the curved micropillars again along the path, and the droplets are driven by means of the recovery of the microcolumn shape (Figs. 2c and d). In addition, perfluoropolyether is immiscible with water and organic solvents, so oil droplets or water droplets can be driven on the micropillar array chip without loss. The magnetic response performance of micropillars mainly depends on the content of reduced iron powder in micropillar. The reduced iron powder was pre-filled in the micro-pits of the PDMS mold and transferred to EVA micropillars during the thermoforming. Considering that the iron powder content in each micropillar is not entirely consistent, we investigated the consistency of the magnetic response of the micropillar array in Supporting information.

Droplet manipulation on an open surface usually requires a lubricating layer coated on the chip surface. The wettability of the lubricating layer should be superior to that of the working liquid, and the lubricating layer and the working liquid are immiscible with each other [24]. In this work, the wettability of water, paraffin oil, and perfluoropolyether on the surface of the micropillar array chip coated with the PVA layer was tested after silanization. Unlike water and paraffin oil, perfluoropolyether can wet the surface of the silanized micropillar array (Fig. S2 in Supporting information). Therefore, perfluoropolyether was coated on the surface of the micropillar array as the lubricating layer.

We demonstrated the manipulation of water droplets on the surface of the micropillar array. Fig. S3a (Supporting information) shows the 2 μL blue water droplet moving along a straight line driven by light (Video S2 in Supporting information). The movement speed of the water droplet is about 0.25 mm/s. Most of the existing discrete droplet manipulation platforms are designed for water droplets, while the research on oil droplet manipulation is less at present. Some chemical reagents or biological samples need to be dispersed in organic solvents, the surface tension of which is much lower than that of water. The contact angle difference between the two sides of the oil droplet induced by the surface morphology gradient is small. A stronger driving force is needed for oil droplets to overcome the contact angle hysteresis [25]. In this strategy, the droplet driving force includes not only the imbalanced surface tension but also the Marangoni force caused by the temperature gradient. The lubricating oil on the chip surface avoids the friction caused by the contact between oil droplets and micropillars. Therefore, even if the surface tension of liquid paraffin is small (about 26.2×10^{-3} N/m), the oil droplet can still be driven. Fig. S3b (Supporting information) shows the light drives the 2 μL yellow paraffin oil droplet to move in a straight line at about 0.1 mm/s (Video S3 in Supporting information). The droplets containing fluorescent dyes were driven on the micropillar array chip,

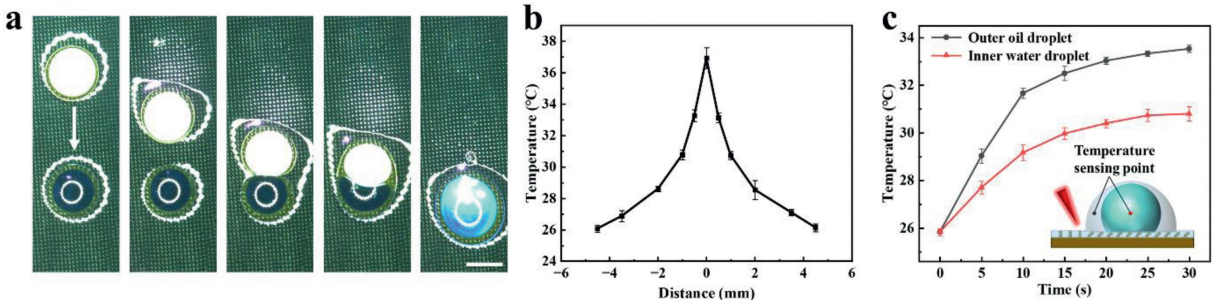

Fig. 3. (a) Images of W/O droplets movement and fusion on the micropillar array chip. Scale bar, 1.5 mm. (b) Temperature change of the lubricating coating around the NIR laser irradiation point. (c) Temperature change of the W/O droplet driven by the NIR laser over time.

and the solutes in water droplets and oil droplets were Rhodamine B and Nile red, respectively. There is no fluorescence in the droplet motion paths. In other words, the solutes in the droplets did not remain on the surface of the chip. This phenomenon is mainly due to the low surface energy of perfluoropolyether coated on the chip surface. (Fig. S5 in Supporting information).

The evaporation of aqueous droplets needs to be avoided since the temperature increases during the light driving. To avoid evaporation of water droplets, we encapsulated water droplets in oil droplets to form double-emulsion droplets with paraffin oil as external phase and water as internal phase (W/O droplets). 0.2% span 80 was added to the paraffin oil to stabilize the double-emulsion system. The oil layer acted as an isolation layer providing a closed environment. We compared the evaporation of aqueous droplets and W/O droplets in an open environment. With the increase of time, the volume of water droplets decreased due to evaporation, while the volume of droplets in W/O had no obvious change (Fig. S6 in Supporting information). The micropillar array chip was placed on an electric heating film. After the W/O droplets were kept at each temperature for 3 min, the temperature of the internal water droplet was measured by a thermocouple thermometer, and its diameter was recorded by a microscope. As shown in Fig. S7 (Supporting information), there is no noticeable change in droplet diameter between 37.1 and 55.1 °C. The outer oil layer can also effectively prevent the evaporation of water droplets at a higher temperature. The results show that the external oil layer prevented the evaporation of water droplets. Fig. 3a shows a white W/O droplet moving in a straight line and merging with a blue W/O droplet on the micropillar array, and a new W/O droplet formed, demonstrating the ability of the proposed platform for manipulating W/O droplets (Video S4 in Supporting information). As shown in Fig. S4 (Supporting information), 0.5 μL W/O droplets are driven to fuse with 5 μL W/O droplets, and then the fused droplets are driven to move along the direction of arrows. The deformation of the micropillar array was based on temperature changes, so the droplets will also be accompanied by temperature changes during movement. We measured the temperature changes of lubricating coating and W/O droplet with a self-made thermocouple thermometer at an ambient temperature of 25.7 °C. The type T thermocouple wire with a diameter of 200 μm was fixed on the three-axis manual sliding table (Zolix), and the position of the thermocouple was controlled by micrometer. The transition temperature of cross-linked EVA was confirmed to be about 50 °C in our previous work [6]. The temperature of lubricating coating on both sides of the NIR laser irradiation point was measured respectively. As shown in Fig. 3b, the temperature change trend on both sides of the zero point is symmetrical. The highest temperature at the irradiation point is 36.9 °C, and the temperature drops rapidly within 2 mm. At 4.5 mm, it is equivalent to room temperature. For W/O droplets (Fig. 3c), the temperature of the outer oil droplets and the inner water droplets increased rapidly within 10 s and reached a

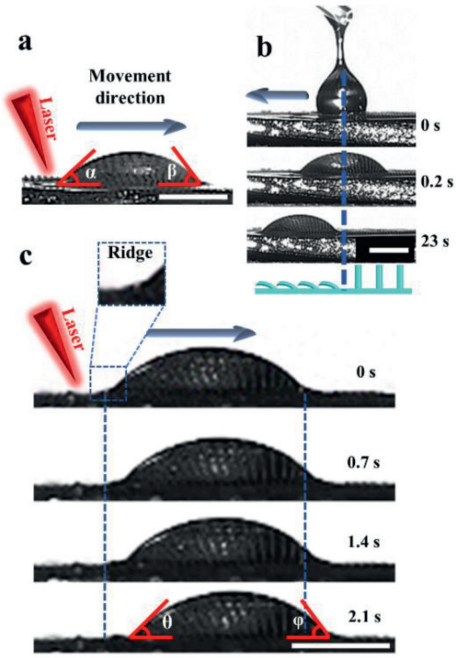

Fig. 4. (a) Image of the moving droplet. (b) The effect of imbalanced surface tension on oil droplet motion. The droplet moved spontaneously from the boundary between vertical micropillar and curved micropillar to the curved micropillar region. (c) Influence of Marangoni effect on oil droplet motion. Scale bars, 1 mm.

stable level after about 20 s. The stable temperatures of outer layer and inner layer are 33.5 and 30.7 °C, respectively. The temperature of the outer oil droplets at the temperature sensing point is always higher than that of the inner water droplets because the outer oil phase slows down the effect of photothermal on the inner water droplets. To sum up, the temperature of lubricating coating, outer oil droplet, and inner water droplet decreased sequentially, and the lubricating coating and outer oil droplet reduced the influence of chip surface temperature changes on inner water droplets.

When the NIR laser scans again along the constructed path, the droplets are driven, and the curved micropillars return to a vertical state after the temperature rising to the transition temperature. The micropillar returning to the vertical state locates at the receding contact angle (RCA) of the droplet, while the micropillar at the advancing contact angle (ACA) is still in a curved state. There is a morphological gradient difference between the micropillars on the two sides of the droplet, resulting in the difference of the contact angles between the two sides. Fig. 4a is a high-speed camera (i-speed TR, Olympus, Japan) shot of a moving droplet, and the ACA (β) of the droplet is from 50° to 54° and the RCA (α) is from 50° to 46°. The surface morphology gradient breaks the surface ten-

sion balance of oil droplets. Thus the oil droplets move forward driven by the imbalanced surface tension [26,27]. Marangoni effect is another droplet driving force owing to the temperature gradient on the chip surface and droplets during droplet manipulation. The temperature gradient will lead to surface tension gradient, and the fluid will flow from low surface tension to high surface tension [28]. In Video S5 (Supporting information), the left side of the oil droplet containing calcium carbonate powder was irradiated by NIR laser, and a temperature gradient was formed from left to right. The convection movement of the fluid in the droplet occurred while the droplet moved forward. In addition, the perfluoropolyether on the chip surface will also generate temperature gradient due to laser irradiation. As shown in Fig. S8 (Supporting information), under the action of the surface tension gradient, the perfluoropolyether coated on the chip surface will diffuse around the laser spot, and the calcium carbonate particles on its surface will move along. Therefore, the flow of the perfluoropolyether on the chip surface can also promote the movement of droplets.

Imbalanced surface tension and Marangoni force exist simultaneously during droplet manipulation. In order to further reveal their effects in droplet driving, we separately investigated their effects on droplet motion. The paraffin oil droplet was added upon the dividing line between the curved micropillars and the vertical micropillars. Only imbalanced surface tension caused by the morphological gradient of the micropillar worked without NIR laser irradiation. In this case, the droplet spontaneously moved to the curved micropillar region under the action of the imbalanced tension, and then stopped after the whole droplet reaching the curved micropillar region (Fig. 4b). Because the surface tension of the oil phase is much smaller than that of water, the paraffin oil droplet moves more slowly than the water droplet (Fig. S9a in Supporting information). When NIR laser irradiated the paraffin oil droplet on the vertical micropillar array, only the Marangoni effect induced by the temperature gradient worked as the driving force. As shown in Fig. 4c, at 0 s, the wetting ridges on the two sides of the droplet were formed by the out-of-plane component of the droplet surface tension acting on the lubricant [29]. With NIR laser irradiation, the perfluoropolyether on the irradiated side diffused, causing the disappearance of the wetting ridge (at 2.1 s). The ACA (φ) of the paraffin oil droplet is from 45° to 47° and the RCA (θ) is from 45° to 43° because of the Marangoni effect. Short displacement of paraffin oil droplet occurs, and the same phenomenon happens to water droplet (Fig. S9b in Supporting information). Either imbalanced surface tension or Marangoni force alone can overcome the resistance to drive the droplet, and they have almost equal effects on the droplet movement.

Surface-enhanced Raman spectroscopy (SERS) is widely used in chemical and biological analysis because of its advantages of non-destructive, *in-situ*, sensitive, and rapid detection. We combined the droplet manipulation platform with a Raman spectrometer to explore an analytical method for minute samples. Rhodamine 6G (Rh6G) was used as the target and AuNPs as the SERS substrate. AuNPs droplets were fused with Rh6G droplets through the proposed droplet manipulation technique. As shown in Fig. 5, due to the accelerated evaporation of water droplets caused by laser irradiation, the concentrations of Rh6G and AuNPs in water droplets increases, and the SERS signal of Rh6G in water droplets gradually rises. However, the SERS signal of the W/O droplets is relatively stable due to the protection of the outer oil layer (Fig. S10 in Supporting information). The combination of droplet manipulation platform and SERS has potential for the analysis of tiny samples.

In summary, we fabricated a magnetic/light dual-response shape-memory micropillar array chip for droplet manipulation. The micropillar array has favorable reusability and good consistency in magnetic response. NIR laser irradiation was used to shape the micropillars in the magnetic field to construct the droplet movement path. NIR laser re-scanning along the path induced the micropillar array to form surface morphology gradient and the droplet to form temperature gradient, and thus the imbalanced surface tension and Marangoni force drove the droplet movement together. The lubricating layer coated on the chip reduces the resistance of droplet movement. This strategy realizes reversible deformation of the micropillars and flexible droplet manipulation. We compared the current common droplet driving methods based on light and magnetic fields and summarized the specific parameters in Table S1 (Supporting information). Our droplet control platform can manipulate not only water droplets but also oil and W/O droplets. In addition, the platform can manipulate tiny droplets (as low as 0.5 μL) because the W/O droplets can prevent the evaporation of small water droplets. The droplet manipulation platform is particularly suitable for micro-reactions involving heating, such as PCR. And it has great potential in constructing bioanalysis systems for tiny samples by combining with a Raman spectrometer or a fluorescence microscope.

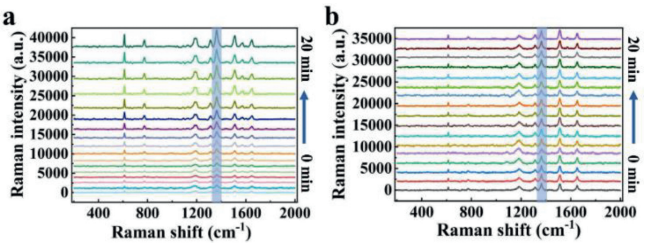

Fig. 5. SERS spectra of Rh6G in water droplet (a) and W/O droplet (b) collected at different time.

Declaration of competing interest

The authors declare that they have no known competing financial interests or personal relationships that could have appeared to influence the work reported in this paper.

Acknowledgments

This work was supported by the Natural Science Foundation of China (No. 21874015) and the Fundamental Research Funds for the Central Universities (No. N2005024).

Supplementary materials

Supplementary material associated with this article can be found, in the online version, at doi:10.1016/j.cclet.2023.108494.

References

[1] Y. Zhang, N.T. Nguyen, Lab Chip 17 (2017) 994–1008.
[2] V. Shukla, F.A. Hussin, N.H. Hamid, N.B. Zain Ali, Sensors 17 (2017) 1719.
[3] A.H. Ng, B.B. Li, M.D. Chamberlain, A.R. Wheeler, Annu. Rev. Biomed. Eng. 17 (2015) 91–112.
[4] K. Han, Z. Wang, L. Heng, L. Jiang, J. Mater. Chem. A 9 (2021) 16974–16981.
[5] C. Gao, L. Wang, Y. Lin, et al., Adv. Funct. Mater. 28 (2018) 1803072.
[6] W.Q. Ye, Y.Y. Wei, D.N. Wang, C.G. Yang, Z.R. Xu, Lab Chip 21 (2021) 1131–1138.
[7] J.K. Park, S. Kim, Lab Chip 17 (2017) 1793–1801.
[8] G. Chen, Z. Dai, S. Li, et al., ACS Appl. Mater. Interfaces 13 (2021) 1754–1765.
[9] A. Lendlein, O.E.C. Gould, Nat. Rev. Mater. 4 (2019) 116–133.
[10] Z. Cheng, D. Zhang, X. Luo, et al., Adv. Mater. 33 (2021) 2001718.
[11] Z. Cheng, D. Zhang, T. Lv, et al., Adv. Funct. Mater. 28 (2018) 1705002.
[12] D. Zhang, Z. Cheng, H. Kang, et al., Angew. Chem. Int. Ed. 57 (2018) 3701–3705.
[13] W. Wang, H. Lai, Z. Cheng, et al., ACS Appl. Mater. Interfaces 12 (2020) 49219–49226.
[14] Y. Shao, W. Du, Y. Fan, et al., Chem. Eng. J. 427 (2022) 131718.
[15] S.H. Yang, J. Park, J.R. Youn, Y.S. Song, Lab Chip 18 (2018) 2865–2872.
[16] B. Aksoy, N. Besse, R.J. Boom, et al., Lab Chip 19 (2019) 608–617.
[17] K. Wang, Y.G. Jia, C. Zhao, X.X. Zhu, Prog. Mater. Sci. 105 (2019) 100572.
[18] M. Zare, M.P. Prabhakaran, N. Parvin, S. Ramakrishna, Chem. Eng. J. 374 (2019) 706–720.

[19] P. Testa, R.W. Style, J. Cui, et al., Adv. Mater. 31 (2019) 1900561.
[20] S.J.M. van Vilsteren, H. Yarmand, S. Ghodrat, Magnetochemistry 7 (2021) 123.
[21] J. Shan, L. Wang, H. Yu, et al., Mater. Sci. Technol. 32 (2016) 602–614.
[22] S.K. Sharma, N. Shrivastava, F. Rossi, L.D. Tung, N.T.K. Thanh, Nano Today 29 (2019) 100795.
[23] M. Villegas, Y. Zhang, N. Abu Jarad, L. Soleymani, T.F. Didar, ACS Nano 13 (2019) 8517–8536.
[24] S. Peppou-Chapman, J.K. Hong, A. Waterhouse, C. Neto, Chem. Soc. Rev. 49 (2020) 3688–3715.
[25] J. Li, Q.H. Lin, A. Shah, et al., Sci. Adv. 2 (2016) e1600148.
[26] S. Daniel, M.K. Chaudhury, J.C. Chen, Science 291 (2001) 633.
[27] Y. Lin, Z. Hu, M. Zhang, et al., Adv. Funct. Mater. 28 (2018) 1800163.
[28] A. Karbalaei, R. Kumar, H. Cho, Micromachines 7 (2016) 13 Basel.
[29] S. Karpitschka, S. Das, M. van Gorcum, et al., Nat. Commun. 6 (2015) 7891.